Complementary Surface-Enhanced Resonance Raman Spectroscopic Biodetection of Mixed Protein Solutions by Chitosan- and Silica-Coated Plasmon-Tuned Silver Nanoparticles

ARTICLE *in* ANALYTICAL CHEMISTRY · JUNE 2012

Impact Factor: 5.64 · DOI: 10.1021/ac301001a · Source: PubMed

6 AUTHORS, INCLUDING:

Arumugam Sivanesan
Queensland University of Technology
30 PUBLICATIONS **310** CITATIONS
SEE PROFILE

Inez M Weidinger
Technische Universität Berlin
49 PUBLICATIONS **551** CITATIONS
SEE PROFILE

analytical chemistry

Article

pubs.acs.org/ac

Complementary Surface-Enhanced Resonance Raman Spectroscopic Biodetection of Mixed Protein Solutions by Chitosan- and Silica-Coated Plasmon-Tuned Silver Nanoparticles

Arumugam Sivanesan,[†] Govindasamy Kalaivani,[†] Anna Fischer,[†] Konstanze Stiba,[‡] Silke Leimkühler,[‡] and Inez M. Weidinger*[,†]

[†]Institut für Chemie, Technische Universität Berlin, Sekr. PC 14, Strasse des 17. Juni 135, D-10623 Berlin, Germany

[‡]Institut für Biochemie und Biologie, Universität Potsdam, Karl-Liebknecht Strasse 24-25, H. 25, Golm, D-14476, Germany

Supporting Information

ABSTRACT: Silver nanoparticles with identical plasmonic properties but different surface functionalities are synthesized and tested as chemically selective surface-enhanced resonance Raman (SERR) amplifiers in a two-component protein solution. The surface plasmon resonances of the particles are tuned to 413 nm to match the molecular resonance of protein heme cofactors. Biocompatible functionalization of the nanoparticles with a thin film of chitosan yields selective SERR enhancement of the anionic protein cytochrome b_5, whereas functionalization with SiO_2 amplifies only the spectra of the cationic protein cytochrome *c*. As a result, subsequent addition of the two differently functionalized particles yields complementary information on the same mixed protein sample solution. Finally, the applicability of chitosan-coated Ag nanoparticles for protein separation was tested by in situ resonance Raman spectroscopy.

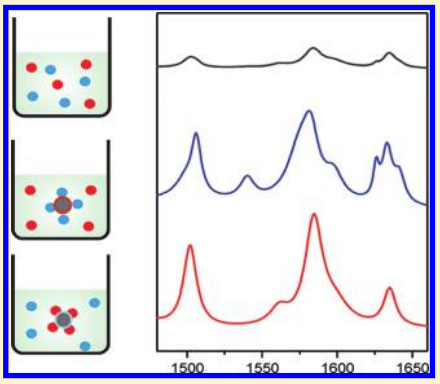

Plasmonic nanoparticles find wide applications in bioanalytical chemistry for detection, discrimination, and diagnosis of biological probes. One of the most common techniques hereby is surface-enhanced Raman (SER) scattering where the resonant coupling of light with the particle's surface plasmons is used to enhance the Raman signal of molecules in close vicinity of the particle surface. The derived vibrational pattern provides highly specific structural information of target molecules; hence, SER spectroscopy is able to discriminate different types of biomolecules or microorganisms such as DNA, proteins, cells, tissues, viruses, or bacteria.[1−7]

The most challenging part in direct SER sensing remains to find suitable characteristics for biomolecule identification as the variation in the vibrational signature within identical samples is rather large and the binding affinities of the nanoparticles to the various target molecules strongly influence the measured spectra.[8,9]

Most of the target-specific SER characterization is therefore done on samples where only one type of target is present, which implies extended purification of mixed sample solutions. However, for any expansion of SER sensing to in vivo systems, where a multitude of target molecules are coexisting, selective sensing systems for one target present in a multicomponent solution need to be developed. The selectivity toward a certain target is in many cases controlled by the nanoparticle surface functionalization; hence, the different binding affinities of the species present in the sample solution can have a strong influence on the SER spectroscopic analysis.[10] Changing the surface properties of the particles can therefore in many cases lead to different spectral identification of the very same sample. A simple and general way to control analyte affinity is achieved by nanoparticle functionalization with charged or polar functional groups. In most of the common protocols for synthesis of colloidal suspensions negatively charged capping agents such as citrate are present at the surface which are incompatible for anionic target molecules and furthermore lead to denaturation of surface-bound biological samples.[11] Therefore, several synthetic approaches have been developed to replace the citrate ions with biocompatible coatings of either positively or negatively charged surface groups.[12−15]

A higher sensitivity for selected target molecules can be introduced for proteins that contain chromophoric cofactors by choosing an excitation line close to the chromophore's absorbance maximum. The so-derived resonance Raman (RR) spectrum not only exceeds the normal Raman spectrum up to several orders of magnitude in intensity but displays the vibrational signature of the protein cofactor only.[16] The combination of surface enhancement by metal nanostructures and resonance Raman effect yields a 2-fold enhanced surface-enhanced resonance Raman (SERR) spectrum of the immobilized proteins.[16−18] The intensity of the SERR spectrum can be optimized by tuning the surface plasmon resonance of the enhancer nanoparticles to a wavelength that matches both

Received: April 16, 2012
Accepted: May 31, 2012
Published: May 31, 2012

   dx.doi.org/10.1021/ac301001a | *Anal. Chem.* 2012, 84, 5759−5764

the laser excitation line and the molecular absorbance maximum.[13,19,20]

Hemes are one of the most common protein cofactors. Hemoproteins carry out a variety of biological functions ranging from biological electron transfer to oxygen transport and enzymatic catalysis. All heme-type chromophores exhibit a strong absorption band around 400 nm making their RR spectra highly visible upon violet light excitation. Although the presence of a heme can be easily detected by UV−vis spectroscopy, further discrimination and analysis relies on spectroscopic techniques that provide more specific information about the direct heme environment. Heme cofactors in different proteins often exhibit a different axial ligation. The type of axial ligand has a strong influence on the vibrational band positions in the marker band region (1300−1700 cm^{-1}), and thus, the different heme species can be discriminated by their respective RR or SERR spectra.[21]

We have recently synthesized Ag nanoparticles with surface plasmon resonances that were tuned to match precisely the absorption maximum of heme cofactors at 413 nm.[13,14] The particles were coated either with carboxylic acid terminated self-assembled monolayers (SAMs) of mercaptoundecanoic acid (Ag@MUA) or with a thin SiO_2 film (Ag@SiO_2) to prevent direct harmful contact between the Ag surface and the protein. Both types of particles were suitable for Raman signal enhancement of the cationic heme protein cytochrome *c* (cyt *c*) while preserving the proteins nativity. The particles, however, were not able to enhance the Raman signal of the anionic heme protein cytochrome b_5 (cyt b_5) most likely due to electrostatic repulsion of the negatively charged nanoparticles (NPs) and the protein.

Chitosan (CS) coatings are widely used in biosensory and biomolecule delivery due to the excellent biocompatibility and biodegradation of chitosan.[22] Furthermore, CS exhibits a high affinity for anionic biomolecules.[23,24] In this work we have therefore synthesized chitosan-functionalized Ag nanoparticles (Ag@CS) that exhibit identical optical properties but complementary binding affinity as compared to Ag@MUA and Ag@SiO_2. We show that these particles can efficiently enhance the Raman signals of cyt b_5. By subsequent addition of either Ag@SiO_2 or Ag@CS NPs we further demonstrate that selective enhancement of a single heme species can be achieved in a heterogeneous protein solution.

EXPERIMENTAL SECTION

Chemicals. Silver nitrate, trisodium citrate, sodium borohydride, ascorbic acid (AA), 3-aminopropyltrimethoxysilane (APTS), sodium silicate solution, and chitosan (medium molecular weight) were obtained from Sigma-Aldrich and used without further purification. All solutions were prepared with Millipore water (18 MΩ, Eschborn, Germany). Horse heart cyt *c* was purchased from Sigma-Aldrich and purified by high-performance liquid chromatography.

Instrumentation. SERR spectra were measured with the 413 nm excitation line of a Kr^+ laser using a confocal Raman microscope (LabRam HR-800, Jobin Yvon) equipped with a N_2(l)-cooled back illuminated charge-coupled device (CCD) detector. The laser beam was focused on the rotating cuvette with a long working distance objective (20× ; numerical aperture 0.35). SERR spectra were acquired with a laser power of 1 mW. UV−vis spectra were collected with a Cary 50 spectrometer. For the transmission electron microscopy (TEM) measurements a drop of the sample solution was deposited on a carbon-coated copper grid for 10 min to allow particle adsorption on the carbon foil. The leftover solution was subsequently removed with a filter paper. TEM measurements were performed on a FEI Tecnai G^2 20 S-TWIN, operated at 200 kV. When required, the deposited sample was stained directly after deposition on the carbon-coated copper grid with a 0.1 wt % H_2WO_4 aqueous solution and subsequently washed with one drop of distilled water.

Synthesis of Colloidal Silver. Small citrate-capped silver nanoparticles (Ag@citrate NPs; d = 12 nm, c_{NP} ∼ 10 nM) were synthesized by reduction of $AgNO_3$ with $NaBH_4$ in the presence of citrate as described previously.[13] These particles were subsequently used as seeds for the synthesis of AgNPs of larger size via the seeding growth method.[13,14]

Chitosan Coating. For the synthesis of chitosan-coated AgNPs (Ag@CS NPs) in aqueous solution with SPR at 413 nm, 50 mL of the AgNPs seed solution was mixed with 1 mL of 1 mM AA, respectively, upon stirring.[25] After 2 min, 1 mL of 1 mM $AgNO_3$ was slowly added under vigorous stirring. The stirring was continued for 1 h. Subsequently 5 mL of freshly prepared 0.1% (w/v) chitosan in 1% (v/v) acetic acid solution was added to 25 mL of seeded AgNPs under hot condition (80−90 °C). The stirring was continued for 3 h, and the NPs were finally stored at 4 °C. In a final washing step the particle solution was concentrated by slow evaporation of the solvent followed by redispersion of the NPs in water.

Silica Coating. For the synthesis of silica-coated AgNPs (Ag@SiO_2 NPs) with SPR at 413 nm, 50 mL of the AgNPs seed solution was mixed with 0.5 mL of 1 mM AA, respectively, upon stirring. After 2 min, 0.5 mL of 1 mM $AgNO_3$ was slowly added under vigorous stirring. The stirring was continued for 1 h. Subsequently, a freshly prepared aqueous solution of 3-aminopropyltriethoxysilane (APTS 0.4 mL, 0.2% (v/v)) was added to 25 mL of seeded AgNPs at pH 5.0. Defect-free coating of the SiO_2 layer was achieved in the second step by adding 2 mL of 2% (v/v) sodium silicate solution. The pH was adjusted to 10.0, and the solution was stirred for 24 h. Finally, the Ag@SiO_2 NPs were purified by centrifugation and redispersed in water before being stored at 4 °C. A more detailed description of the Ag@SiO_2 NP synthesis is given in ref 14.

Cloning, Expression, and Purification of Cytochrome b_5 Domain from Human Sulfite Oxidase. The published gene sequence of human sulfite oxidase (hSO)[26] was used to design primers that permitted cloning of the gene sequence corresponding to the N-terminal cyt b_5 domain of hSO into the NdeI and *Eco*RI sites of the pET15b expression vector. The resulting plasmid was designated pKS1 and expresses hSO-b5 as an N-terminal fusion protein with a His6-tag. For heterologous expression in *Escherichia coli*, BL21(DE3) cells were transformed with pKS1. To express recombinant proteins, 4 L cultures of BL21(DE3) × pKS1 cells were grown in LB medium containing ampicillin to an A600 of 0.6 and subsequently induced by the addition of 0.1 mM isopropyl-β-D-thiogalactopyranoside. After 4−6 h of aerobic growth at 30 °C, the cells were harvested and resuspended with a total of 40 mL of 50 mM NaH_2PO_4, 300 mM NaCl, pH 8.0. Complete cell lysis was achieved by three passages through a TS series benchtop cell disruptor (Constant Systems, Daventry, U.K.) at 1350 bar in the presence of DNaseI (1 μg/mL). The resulting extract was centrifuged at 20 000*g*. The cleared lysate was applied to 1.5 mL of Ni^{2+}−nitrilotriacetic acid (Qiagen, Hilden, Germany) per liter of culture. The column was washed with 2

dx.doi.org/10.1021/ac301001a | *Anal. Chem.* 2012, 84, 5759−5764

× 20 column volumes of phosphate buffer containing 10 and 20 mM imidazole each. Protein was eluted with phosphate buffer containing 250 mM imidazole, and the buffer was changed to 100 mM Tris, 1 mM EDTA, pH 8.5 by either dialysis or G25 size exclusion chromatography (PD10, GE Healthcare, Munich, Germany).

RESULTS AND DISCUSSION

Characterization of Chitosan-Coated Ag Nanoparticles. Small Ag NPs (d = 10−12 nm) exhibiting a surface plasmon resonance at 394 nm[13] were used as seeds for the synthesis of larger and more ellipsoidal particles upon addition of $AgNO_3$ and AA. The concentrations of $AgNO_3$ and AA were chosen so that the surface plasmon resonance (SPR) of the seeded Ag@citrate NPs was shifted to 407 nm. Surface functionalization with chitosan, which was achieved by stirring the seeded particles in a chitosan-containing solution, resulted in a further SPR red shift of 4−6 nm. The UV−vis spectrum of the Ag@CS particle solution is shown in Figure 1C. It can be seen that the SPR was precisely tuned to 413 nm, which is in resonance with the incoming laser light and the absorption maximum of a heme chromophore.[17] Also shown in Figure 1C is the UV−vis spectrum of $Ag@SiO_2$ NPs that were previously synthesized and which were also tuned to an SPR maximum of 413 nm. From Figure 1C it becomes clear that both types of particles exhibit identical optical properties.

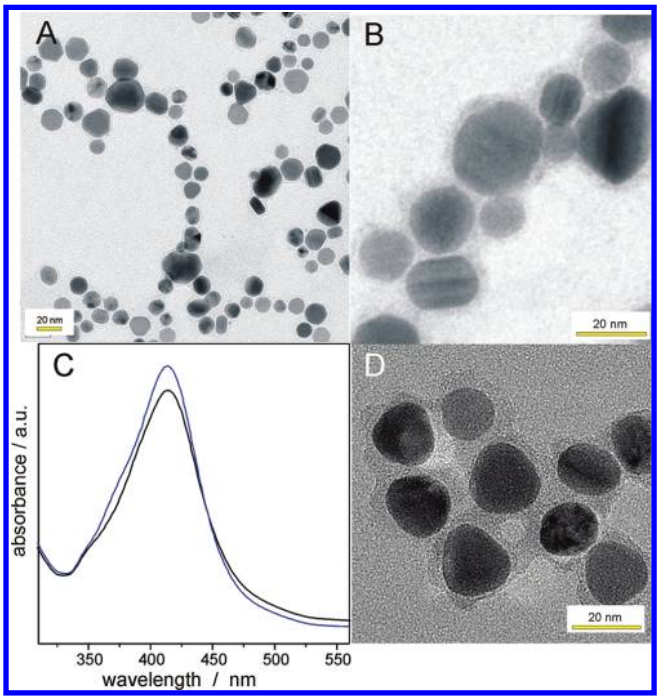

Figure 1. (A) TEM picture of Ag@CS nanoparticles. (B) TEM of Ag@CS after staining the chitosan coating with a 0.1 wt % H_2WO_4 aqueous solution. (C) UV−vis absorption spectrum of Ag@CS (blue) and $Ag@SiO_2$ (black) NPs. (D) TEM picture of $Ag@SiO_2$ NPs.

TEM pictures of chitosan-coated AgNPs with SPR maximum around 413 nm are shown in Figure 1, parts A and B. The mean diameter of the Ag@CS NPs was determined to be 19 ± 5 nm. Staining of Ag@CS NPs with an aqueous solution of H_2WO_4 clearly evidences the chitosan coating around the NPs (Figure 1B), and the average thickness of the CS layer was determined to be 3.5 ± 1 nm. In Figure 1D a TEM picture of the $Ag@SiO_2$ NPs is shown for comparison. The average particle diameter (d = 18 ± 4) and SiO_2 coating thickness (4 ± 2 nm) were found to be comparable to those of the Ag@CS particles. Hence, the only significant difference between these two types of particles relates to their functional surface groups which consist of −OH groups in the case of SiO_2 and $-NH_2$ groups in the case of CS. The properties of both NP ensembles are summarized in Table 1.

Table 1. Properties of $Ag@SiO_2$ and Ag@CS Nanoparticles

	$Ag@SiO_2$	Ag@CS
$d_{particle}$	18 ± 4 nm	19 ± 5 nm
$d_{coating}$	4 ± 2 nm	3.5 ± 1 nm
SPR_{max}	413 nm	413 nm
REF_{413}	400	1200
sensitivity	cyt c	cyt b_5
Γ_{max}	1.2 μM	0.15 μM

SERR Spectroscopy of Heme Proteins. Two types of heme proteins, cyt c and cyt b_5 (Figure 2), were chosen as biomolecular Raman probes for testing the target-specific enhancement of Ag@CS and $Ag@SiO_2$ NPs. Cytochrome b_5 occurs in nature as a subunit of hSO, an enzyme that catalyzes the oxidation of sulfite to sulfate and thus plays a crucial role in sulfite detoxification in the human organism. The two electrons that are generated upon sulfite oxidation at the catalytic molybdenum cofactor (Moco) center are transferred via the cyt b_5 unit to the external redox partner cyt c.[27,28] Both proteins exhibit a single heme redox center that is responsible for their strong Soret-band absorption around 400 nm; thus, it is difficult to distinguish them by their absorbance profile. However, cyt c and cyt b_5 exhibit different axial heme ligations, as the sixth ligand is a methionine in the case of heme c in cyt c and a histidine for heme b of cyt b_5 (Figure 2, parts C and D).

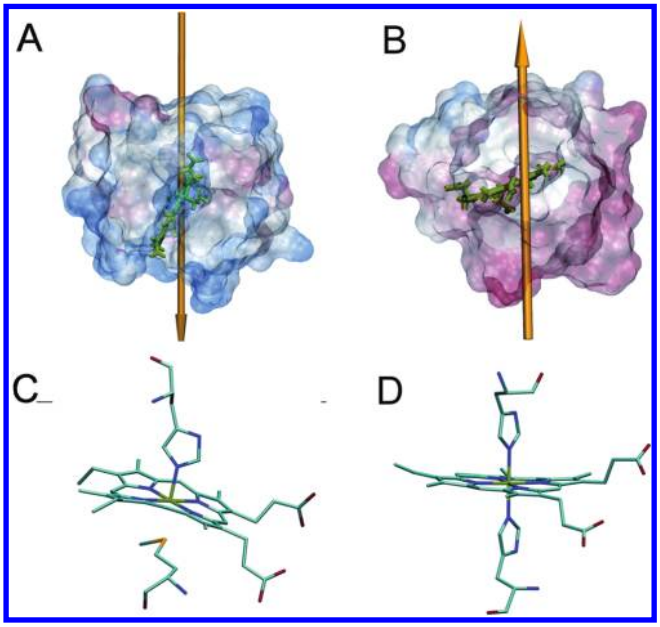

Figure 2. Calculated surface charge distribution and dipole moments of cyt c (A) and cyt b_5 (B). Axial ligation of heme c in cyt c (C) and heme b in cyt b_5 (D). The pictures were adapted from refs 30 and 17. Positively charged amino acid residues are depicted in blue, negatively charged are in red.

dx.doi.org/10.1021/ac301001a | Anal. Chem. 2012, 84, 5759−5764

As a result the band positions and relative band intensities in the frequency region between 1300 and 1700 cm^{-1} of the respective RR spectra are slightly different[17,29] (Figure 3, parts A and B). Thus, it is possible to discriminate cyt *c* and cyt b_5 by RR spectroscopy. The most significant difference between the two proteins lies in their surface charge distribution and dipole moment (Figure 2, parts A and B).[17,30] By looking at the protein side with the exposed heme group one can see that cyt b_5 exhibits a negative net surface charge, whereas cyt *c* is clearly positively charged. The dipole moment of the protein controls its electrostatic interaction with nanoparticles; hence, it is expected that cyt *c* and cyt b_5 bind to particles with complementary surface charge. We have shown in a previous work that the SERR signal of cyt *c* could be greatly enhanced by adding Ag@SiO_2 NPs to the solution (Figure 3, parts B and D).[14] Adding the same Ag@SiO_2 particles to a cyt b_5 solution did not result in signal enhancement due to electrostatic repulsion of the particle and the protein.

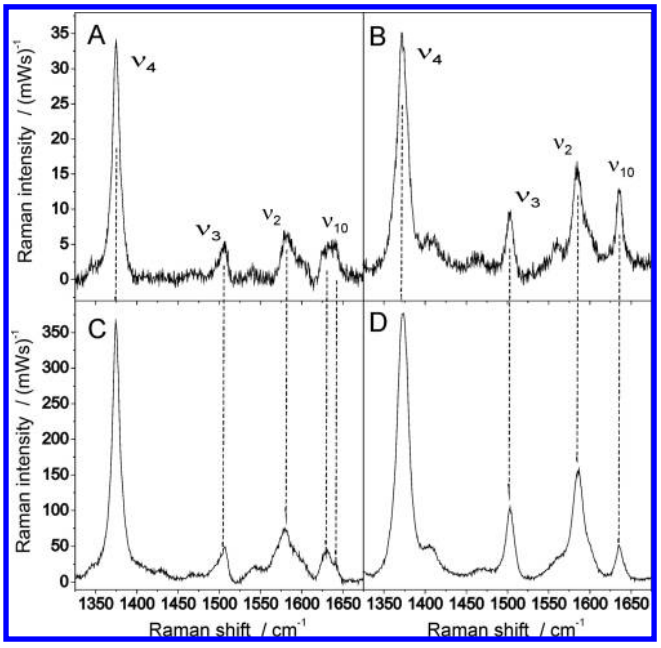

Figure 3. (A) RR spectrum of cyt b_5 (5 μM) in solution and with Ag@CS NPs (C). (B) RR spectrum of cyt *c* (20 μM) in solution and with Ag@SiO_2 NPs (D).

However, a signal enhancement of cyt b_5 could be observed upon Ag@CS NP addition (Figure 3C). The band positions of the RR (Figure 3A) and SERR (Figure 3C) spectra of ferric cyt b_5 are identical confirming that the nativity of the heme pocket is preserved upon interaction with the Ag@CS NPs. The preservation of nativity of cyt b_5, however, depends on the thickness and homogeneity of the chitosan coating. Indeed, using Ag@CS particles as enhancers synthesized with a low concentration (0.004% (w/v) chitosan) of CS during the coating step results in the appearance of a new band at 1491 cm^{-1} (Supporting Information Figure S2). This band is generally attributed to a nonnative five-coordinated high-spin species. This denaturation of the protein might result from an incomplete CS coating, allowing proteins to directly interact with the Ag surface. Under our experimental conditions a chitosan concentration of 0.017% (w/v) was found to be sufficient for obtaining SERR spectra that correspond to the native state of the protein; hence, we assume that for this concentration a complete CS layer has been formed. However, the preservation of protein nativity has been achieved at the expense of SERR intensity that drops to 15% of its initial value directly on Ag due to the larger separation of the protein from the Ag surface.

The vibrational spectra of native cyt b_5 show a predominant band (ν_4) at 1374 cm^{-1} which is used in the following as a reference band to determine the Raman enhancement factor (REF) at the Ag@CS surface. REF can be calculated by the following equation:

$$\mathrm{REF} = \frac{I_{\mathrm{SERR}} c_{\mathrm{RR}}}{I_{\mathrm{RR}} c_{\mathrm{SERR}} k} \quad (1)$$

For I_{RR} the Raman intensity of cyt b_5 for c_{RR} = 5 μM was taken. The concentration of surface-bound cyt b_5 (c_{SERR}) in the saturation limit was estimated as 0.154 μM based on a previously published procedure.[11,13] *k* is a shielding factor determined in previous work to be 0.25. The factor I_{SERR}/I_{RR} = 9.2 was determined from the difference in Raman intensity of cyt b_5 in the presence and absence of NPs. Accordingly, REF was found to be 1200. This value is 3 times higher than the one determined for Ag@SiO_2 NPs in a previous work (see Table 1). This result can be rationalized if partial penetration of the protein into the chitosan layer is assumed. The actual distance of the protein to the Ag surface would then be actually smaller than the estimated 3.5 nm chitosan layer thickness.

Selective SERR Enhancement. To finally test the selective sensitivity of Ag@CS and Ag@SiO_2 NPs in heterogeneous samples both differently functionalized nanoparticles were successively added to a separate solution each containing a mixture of cyt *c* and cyt b_5. The RR spectrum of a mixed cyt *c*/cyt b_5 solution of ratio 4:1 is shown in Figure 4A. Component analysis, using the respective RR spectra of pure cyt *c* and cyt b_5 solutions from Figure 3, parts A and B, showed almost equal

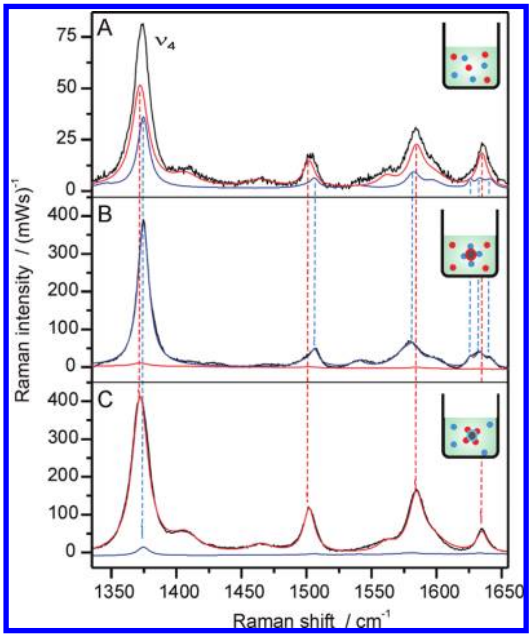

Figure 4. (A) RR spectra of a 1:4 mixture of cyt b_5 (5 μM) and cyt *c* (20 μM). The fitted component spectra of cyt b_5 and cyt *c* are depicted in blue and red, respectively. (B) SERR spectrum of the 1:4 cyt b_5 + cyt *c* mixture with Ag@SiO_2 NPs. (C) SERR spectrum of the 1:4 cyt b_5 + cyt *c* mixture with Ag@CS (C) NPs.

dx.doi.org/10.1021/ac301001a | *Anal. Chem.* 2012, 84, 5759−5764

spectral contributions of both proteins to the measured spectrum. It is therefore concluded that the Raman cross section of cyt b_5 is 4 times higher than that of cyt *c*. The SERR spectrum recorded after addition of Ag@CS is shown in Figure 4B. This spectrum can almost completely be fitted using solely the component spectrum of cyt b_5 from Figure 3D alone. The opposite effect was observed if Ag@SiO_2 NPs were added to the mixture (Figure 4C). Here only the cyt *c* species contributed to the measured SERR spectrum. Hence, the excellent selectivity of the NPs toward a single heme species could be demonstrated.

Protein Separation. Finally, the separation efficiency of Ag@CS nanoparticles was monitored in situ by RR spectroscopy. In Figure 5A the RR spectrum of a 1:1 cyt b_5–cyt *c*

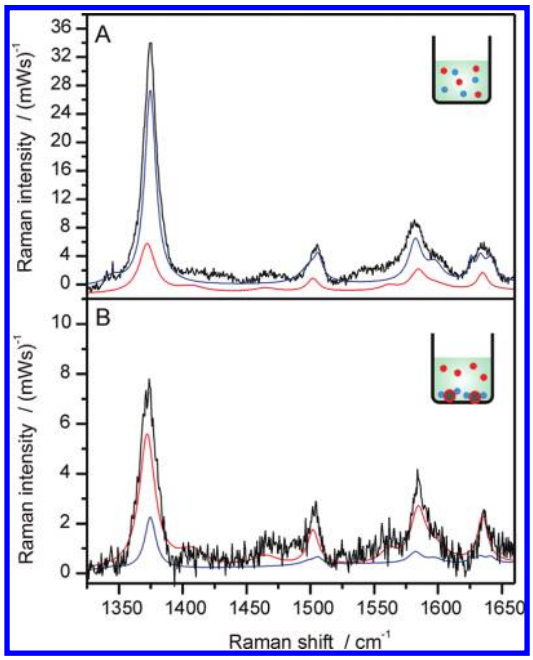

Figure 5. (A) RR spectrum of a 1:1 mixture of cyt b_5 and cyt *c* (2.5 μM). The fitted component spectra of cyt b_5 and cyt *c* are depicted in blue and red, respectively. (B) RR spectrum together with the fitted component spectra of the same solution after Ag@CS NPs have been added and removed.

solution is depicted. Due to its 4 times higher Raman cross section the spectrum of the mixed sample is dominated by the vibrational pattern of cyt b_5. Ag@CS NPs were added to the solution and centrifuged away afterward. The RR spectrum of the remaining solution is shown in Figure 5B. Component analysis revealed only minor changes of the cyt *c* signal intensity, whereas the intensity of the cyt b_5 RR signal decreased by more than 1 order of magnitude. The mixed solution after protein separation by Ag@CS NPs had a cyt *c*/cyt b_5 ratio of 10:1. We can thus conclude that the binding strength between cyt b_5 and Ag@CS is strong enough to separate the two heme species. In contrary a much lower binding force was observed previously for cyt *c* and Ag@SiO_2 NPs. In a similar experiment, in which Ag@SiO_2 NPs were added to a cyt *c* containing solution and subsequently centrifuged away, no change in protein concentration was observed before and after the NPs were added.[14]

CONCLUSION

In this work we have shown that plasmonic Ag nanoparticles with identical optical properties but different surface functionalization can selectively detect, bind, and separate a single heme species in the presence of other heme-type proteins. Upon addition of Ag@SiO_2 or Ag@CS NPs to a heterogeneous cyt *c*/cyt b_5 protein solution almost exclusively the SERR spectrum of either the cationic cyt *c* or the anionic cyt b_5 is enhanced. The observed selective enhancement is a consequence of the complementary binding affinity of the two proteins toward the −OH and $-NH_2$ functional groups of SiO_2 and CS, respectively. The interaction of CS with cyt b_5 did not alter the heme pocket structure, which demonstrates the high biocompatibility of CS. The selective affinity of Ag@CS to cyt b_5 was further used for protein separation. One cycle of adding and removing Ag@CS to a 1:1 cyt b_5/cyt *c* solution leads to a decrease in cyt b_5 concentration of 1 order of magnitude, while cyt *c* remained completely unaffected by the washing process.

The work presented here can be seen as a contribution in establishing a multiplexed analytical method based on biocompatible NPs with different protein binding affinities. This method would allow accumulating much more information of an unknown sample solution than using a single type of NP for analysis. The combination of optical enhancement and controlled surface functionalization furthermore facilitates detection of species with lower concentration or optical sensitivity.

ASSOCIATED CONTENT

Supporting Information

Size distribution of the CS coating thickness and SERR spectra of cyt b_5 on Ag@CS NPs with a low CS coating. This material is available free of charge via the Internet at http://pubs.acs.org.

AUTHOR INFORMATION

Corresponding Author

*E-mail: i.weidinger@mailbox.tu-berlin.de.

Notes

The authors declare no competing financial interest.

ACKNOWLEDGMENTS

The authors thank Peter Hildebrandt for his encouragement and support and Tillmann Utesch for making the pictures in Figure 2. We also thank Dr. Markus Wollgarten from the Helmholtz Zentrum Berlin for access to the TEM facility and fruitful discussions. Financial support by the DFG (Unicat), the Fonds der Chemie, and ILB (TERAsens) is gratefully acknowledged.

REFERENCES

(1) Bell, S. E. J.; Sirimuthu, N. M. S. *J. Am. Chem. Soc.* **2006**, *128*, 15580–15581.
(2) Hermelink, A.; Brauer, A.; Lasch, P.; Naumann, D. *Analyst* **2009**, *134*, 1149–1153.
(3) Millo, D.; Harnisch, F.; Patil, S. A.; Ly, H. K.; Schroder, U.; Hildebrandt, P. *Angew. Chem., Int. Ed.* **2011**, *50*, 2625–2627.
(4) Yang, X.; Gu, C.; Qian, F.; Li, Y.; Zhang, J. Z. *Anal. Chem.* **2011**, *83*, 5888–5894.
(5) Han, X. X.; Kitahama, Y.; Itoh, T.; Wang, C. X.; Zhao, B.; Ozaki, Y. *Anal. Chem.* **2009**, *81*, 3350–3355.
(6) Tang, H. W.; Yang, X. B. B.; Kirkham, J.; Smith, D. A. *Appl. Spectrosc.* **2008**, *62*, 1060–1069.

(7) Aydin, O.; Altas, M.; Kahraman, M.; Bayrak, O. F.; Culha, M. *Appl. Spectrosc.* **2009**, *63*, 1095−1100.
(8) Alvarez-Puebla, R. A.; Arceo, E.; Goulet, P. J. G.; Garrido, J. J.; Aroca, R. F. *J. Phys. Chem. B* **2005**, *109*, 3787−3792.
(9) Alvarez-Puebla, R. A.; Liz-Marzan, L. M. *Small* **2010**, *6*, 604−610.
(10) Alvarez-Puebla, R. A.; Liz-Marzan, L. M. *Chem. Soc. Rev.* **2012**, *41*, 43−51.
(11) Hildebrandt, P.; Stockburger, M. *J. Phys. Chem.* **1986**, *90*, 6017−6024.
(12) Alvarez-Puebla, R. A.; Aroca, R. F. *Anal. Chem.* **2009**, *81*, 2280−2285.
(13) Sivanesan, A.; Ly, H. K.; Kozuch, J.; Sezer, M.; Kuhlmann, U.; Fischer, A.; Weidinger, I. M. *Chem. Commun.* **2011**, *47*, 3553−3555.
(14) Sivanesan, A.; Kozuch, J.; Ly, H. K.; Kalaivani, G.; Fischer, A.; Weidinger, I. M. *RSC Adv.* **2012**, *2* (3), 805−808.
(15) dos Santos, D. S.; Goulet, P. J. G.; Pieczonka, N. P. W.; Oliveira, O. N.; Aroca, R. F. *Langmuir* **2004**, *20*, 10273−10277.
(16) Siebert, F.; Hildebrandt, P. *Vibrational Spectroscopy in Life Science*; Wiley-VCH: Weinheim, Germany, 2008.
(17) Sezer, M.; Spricigo, R.; Utesch, T.; Millo, D.; Leimkuehler, S.; Mroginski, M. A.; Wollenberger, U.; Hildebrandt, P.; Weidinger, I. M. *Phys. Chem. Chem. Phys.* **2010**, *12*, 7894−7903.
(18) Feng, J. J.; Gernert, U.; Hildebrandt, P.; Weidinger, I. M. *Adv. Funct. Mater.* **2010**, *20*, 1954−1961.
(19) Moula, G.; Aroca, R. F. *Anal. Chem.* **2011**, *83*, 284−288.
(20) Witlicki, E. H.; Andersen, S. S.; Hansen, S. W.; Jeppesen, J. O.; Wong, E. W.; Jensen, L.; Flood, A. H. *J. Am. Chem. Soc.* **2010**, *132*, 6099−6107.
(21) Oellerich, S.; Wackerbarth, H.; Hildebrandt, P. *J. Phys. Chem. B* **2002**, *106*, 6566−6580.
(22) Felt, O.; Buri, P.; Gurny, R. *Drug Dev. Ind. Pharm.* **1998**, *24*, 979−993.
(23) Peng, L.; Wollenberger, U.; Kinne, M.; Hofrichter, M.; Ullrich, R.; Scheibner, K.; Fischer, A.; Scheller, F. W. *Biosens. Bioelectron.* **2010**, *26*, 1432−1436.
(24) Orelma, H.; Filpponen, I.; Johansson, L. S.; Laine, J.; Rojas, O. J. *Biomacromolecules* **2011**, *12*, 4311−4318.
(25) Potara, M.; Jakab, E.; Damert, A.; Popescu, O.; Canpean, V.; Astilean, S. *Nanotechnology* **2011**, *22*, 135101.
(26) Garrett, R. M.; Bellissimo, D. B.; Rajagopalan, K. V. *Biochim. Biophys. Acta* **1995**, *1262*, 147−149.
(27) Garrett, R. M.; Johnson, J. L.; Graf, T. N.; Feigenbaum, A.; Rajagopalan, K. V. *Proc. Natl. Acad. Sci. U.S.A.* **1998**, *95*, 6394−6398.
(28) Utesch, T.; Mroginski, M. A. *J. Phys. Chem. Lett.* **2010**, *1*, 2159−2164.
(29) Hu, S. Z.; Morris, I. K.; Singh, J. P.; Smith, K. M.; Spiro, T. G. *J. Am. Chem. Soc.* **1993**, *115*, 12446−12458.
(30) Feng, J. J.; Murgida, D. H.; Kuhlmann, U.; Utesch, T.; Mroginski, M. A.; Hildebrandt, P.; Weidinger, I. M. *J. Phys. Chem. B* **2008**, *112*, 15202−15211.